

See discussions, stats, and author profiles for this publication at: <https://www.researchgate.net/publication/21111766>

# Solution structure of salmon calcitonin

ARTICLE *in* BIOPOLYMERS · FEBRUARY 1991

Impact Factor: 2.39 · DOI: 10.1002/bip.360310210 · Source: PubMed

---

CITATIONS

52

---

READS

11

4 AUTHORS, INCLUDING:



Jean-Philippe Meyer

Evolva Holding

21 PUBLICATIONS 463 CITATIONS

SEE PROFILE



Vladimir Saudek

University of Cambridge

107 PUBLICATIONS 7,246 CITATIONS

SEE PROFILE

# Solution Structure of Salmon Calcitonin

JEAN-PHILIPPE MEYER, JOHN T. PELTON, JAN HOFLACK, and VLADIMIR SAUDEK

Merrell Dow Research Institute, 16 rue d'Ankara, 67000 Strasbourg, France

## SYNOPSIS

Salmon calcitonin, a 32-residue peptide with a 1–7 disulfide bridge, was synthesized by standard solid-phase techniques, and studied by CD and two-dimensional NMR experiments. The peptide was dissolved in pure trifluoroethanol (TFE) and in aqueous solutions containing various amounts of TFE. CD studies in pure TFE indicated the presence of an  $\alpha$ -helical structure comprising 40% of the constituent amino acids. This was fully confirmed by nmr. A detailed analysis was performed with the peptide in a 9 : 1 deuterated TFE/H<sub>2</sub>O mixture. A total of 365 nuclear Overhauser enhancements (154 intraresidual, 112 sequential and 99 long range) were compiled from the nuclear Overhauser enhancement spectroscopy spectra and used in the distance geometry calculations. The core of the peptide between residues 8 and 22 assumes an  $\alpha$ -helix like structure. The Cys 1–Cys 7 ring is well defined and in close association with the helix, while the C-terminal decapeptide folds back toward the core, forming a loose loop.

## INTRODUCTION

Calcitonin is a cyclic 32 amino acid peptide that is synthesized and stored by the parafollicular cells of the thyroid, parathyroid, and thymus glands. Calcitonin's release is mediated by an increase in cyclic AMP production in response to a rise in the calcium concentration in the blood. The principal mode of action of this peptide is inhibition of bone resorption<sup>1</sup> by regulating both the number and activity of osteoclasts. This activity is antagonistic to that of parathyroid hormone. Calcitonins from many different species have been obtained and sequenced since its first isolation and characterization in 1968. Although there are many differences in individual amino acids in calcitonins from different species, they all consist of 32 amino acids, they all have a disulfide bridge between cysteine residues at positions 1 and 7, and the carboxyl terminus is always proline amide. In general, fish calcitonins have been found to be more potent biologically than mammalian ones, and numerous analogues have been studied to better understand the relationship between structure and biological activity. CD studies<sup>2,3</sup> coupled with various predictive methods<sup>4</sup> have sug-

gested that calcitonin assumes a structure containing a loop, involving the disulfide bridge between the cysteines residues, an amphiphilic  $\alpha$ -helix from residues 10 to 20, and a hydrophilic random coil sequence comprising residues 22–32. However, a recent <sup>1</sup>H-nmr study in 90% DMSO–10% H<sub>2</sub>O<sup>5</sup> indicated that an extended conformation was the dominant feature with only short double-stranded antiparallel  $\beta$ -sheet regions and no evidence of a regular helical segment. To better understand the conformational features of salmon calcitonin in solution, we have examined both the CD and <sup>1</sup>H-nmr spectral properties of this peptide in the presence and absence of the structure-promoting solvent trifluoroethanol (TFE). Such a study may provide clues to the structure of the peptide after interaction with a membrane or receptor. We present here the complete sequence-specific assignment of the <sup>1</sup>H-nmr spectrum and a three-dimensional structure derived from these data based on distance geometry calculations.

## MATERIAL AND METHODS

### Peptide Synthesis

Salmon calcitonin was synthesized by standard solid phase synthetic techniques<sup>6,7</sup> using an automated

peptide synthesizer employing Boc/Bzl chemistry and *p*-methylbenzhydrylamine resin (0.51 mmol/g). The peptide was deprotected and removed from the resin with the two-step "low and high" HF method,<sup>8</sup> and was purified by gel filtration on a Sephadex G25 column and preparative C18 reverse-phase high performance liquid chromatography (HPLC).

The resulting product was then characterized by analytical HPLC, thin layer chromatography, and fast atom bombardment mass spectroscopy ( $MH^+$  calculated = 3432.9,  $MH^+$  measured = 3432.9). Amino acid analysis after acid hydrolysis gave the proper molar ratios ( $\pm 9.0\%$ ) of the constituent amino acids. Amino acid sequencing by automated gas phase Edman degradation gave the correct sequence.

### Circular Dichroism

CD studies were performed with an Aviv Model 62D spectropolarimeter in aqueous solutions containing 0–95% TFE, or in pure TFE. The concentration was about 1 mM. Spectra were recorded at 37°C at pH 2.1 (no correction for isotopic effect), using a 1.5-nm bandwidth, 0.5-nm step, and a time constant of 4 s. A total of 5 scans were averaged for both sample and solvent. After correction of the sample spectrum for solvent contributions, the data were fitted by nonlinear regression analysis. Circular cells with a 0.183-mm path length, measured by an ir spectrometer,<sup>9</sup> were used. The estimation of the secondary structure was made using the Aviv program PROSEC (PROtein SECondary structure estimator).

### NMR Spectroscopy and Distance Geometry Calculations

The peptide was dissolved in fully deuterated TFE (TFE-d) containing varying amounts of H<sub>2</sub>O. The concentration was about 4 mM, pH 2.1 (no correction for isotopic effect). The chemical shift was referenced to an internal standard [sodium (3-(trimethylsilyl) [2,2',3,3']-d<sub>4</sub> propionate)].

All spectra were acquired at 37°C on a Bruker AM 500 MHz spectrometer equipped with an Aspect 3000 computer and a digital phase shifter. A set of standard<sup>10</sup> two-dimensional spectra was accumulated in the phase-sensitive mode using time-proportional phase incrementation: double quantum filtered correlated spectroscopy (COSY),<sup>11</sup> homonuclear Hartman–Hahn (HOHAHA),<sup>12</sup> and nuclear Overhauser enhancement spectroscopy (NOESY).<sup>13</sup> The NOE buildup was followed in the NOESY

spectra with mixing times ranging from 100 to 600 ms. The increase of NOE intensities was found to be nearly linear up to 500 ms. The intramolecular distances were deduced from the spectra obtained with 100, 200, and 300 ms using an empirical calibration of 2.6, 3.8, and 5.0 Å for strong, medium or weak NOE, respectively. HOHAHA experiments used a radiofrequency field strength of 7 KHz for spin locking with mixing times of 30 and 120 ms. Water in aqueous solutions was suppressed by saturation during the relaxation delay and, in NOESY experiments, during the mixing time. Data were accumulated using 32 transients and 4 dummy transients in 2K data points in the second time domain ( $t_2$ ) and in 512 in the first ( $t_1$ ). Transmitter offset was placed either in the middle of the spectrum or on the water peak in aqueous solutions. A spectral width of 4.5 KHz and incrementation of 110  $\mu$ s in  $t_1$  were applied. Data were processed off-line on a Bruker X32 station, using the manufacturer's UXNMR program. Free induction decays were multiplied by a Gaussian weighting function and a cosine-bell function in  $t_2$  and  $t_1$ , respectively. Zero filling led to a digital resolution of 2.20 and 4.40 Hz/point in the second ( $F_2$ , horizontal axes of spectra) and the first frequency domain ( $F_1$ , vertical axes of spectra), respectively. The baseline was fitted with a third-degree polynomial in both directions and subtracted from the spectrum. Distance geometry calculations were performed with the program DISMAN. The Brookhaven Protein Database notation is used for the hydrogen atoms.

## RESULTS

### Circular Dichroism

When dissolved in aqueous solutions containing as little as 15% TFE or in pure TFE, salmon calcitonin displays a strong  $\alpha$ -helical character<sup>14</sup> (Figure 1), as shown by the two negative bands at 222 and 207 nm and a positive band at about 194 nm. Nevertheless, the intensity of the minimum at 222 nm is less than expected for a pure  $\alpha$ -helix<sup>14</sup> and the peaks are somewhat broader, indicating the presence of other secondary structural features. The theoretical CD spectrum derived from the PROSEC analysis of the experimental data fits the spectrum in pure TFE well, and predicts that salmon calcitonin is 40%  $\alpha$ -helical, 40%  $\beta$ -pleated sheet, and 20% random coil. However, these results should be taken cautiously, due to the low-intensity signal given by the  $\beta$ -pleated sheet with respect to the  $\alpha$ -helix.

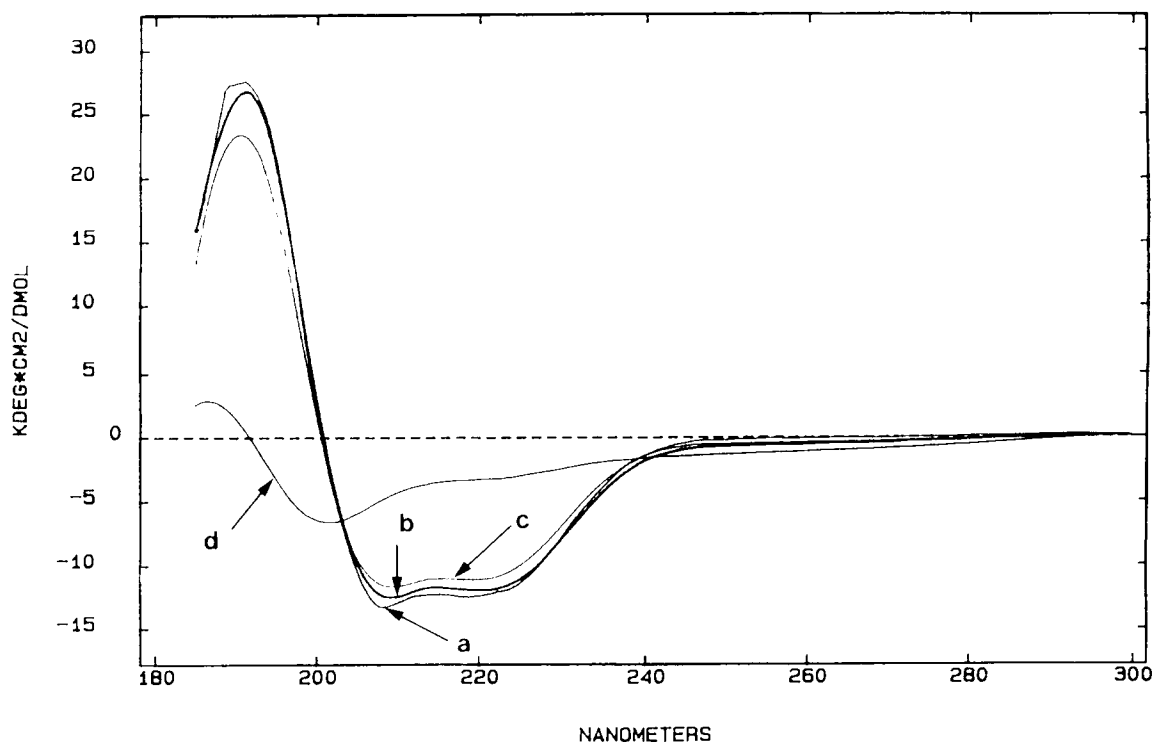


**Figure 1.** CD spectra of salmon calcitonin in (a) pure TFE, (b) 75% TFE, (c) 25% TFE, and (d) pure water.

In pure water, or in aqueous solutions containing less than 15% of TFE, there is a drastic loss of structure, as determined by CD. Salmon calcitonin assumes a nearly random coil conformation, although a small positive maximum in the far uv indicates that there is still some structure left in the peptide. This could be due to the Cys 1–Cys 7 ring system that might, even in water, retain a certain preferred conformation. The presence of an isobestic point at about 203 nm indicates that salmon calcitonin is in equilibrium between two forms, one being mainly  $\alpha$ -helical and the other random coil. No significant changes in the CD spectra of salmon calcitonin in pure TFE were observed during variable pH (pH 2.1–7.4) or temperature (4–60°C) experiments (data not shown).

### Nuclear Magnetic Resonance

**Effects of TFE.** COSY, HOHAHA, and NOESY spectra were accumulated with the peptide in various TFE-d/H<sub>2</sub>O mixtures. Both NOESY and COSY amide regions are much simpler in pure TFE-d (spectra not shown), where many of the amide protons are exchanged with deuterons coming from the

solvent (deuterated alcohol group). The nonexchanged protons are apparently stabilized by the secondary structure. The aliphatic region was very similar in different solvent mixtures, although the chemical shifts changed slightly. The greatest difference was observed in the 3.5–4.0-ppm region, in which minor peaks appeared upon addition of H<sub>2</sub>O. The same effect was observed for the single tyrosine residue (Tyr 22) that displayed two aromatic peaks that split in aqueous solutions. This is attributed to *cis/trans* isomerization of the neighboring proline. The *cis* conformation was estimated from the one-dimensional spectrum to be about 10% in a 9 : 1 TFE-d/H<sub>2</sub>O solution.

We then monitored the HN/HN region in the NOESY spectrum of the peptide as the amount of TFE-d was decreased to 5%, in order to see if the structure was preserved. In the 1 : 1 TFE-d/H<sub>2</sub>O mixture, all HN<sub>*i*</sub>/HN<sub>*i*+1</sub> NOEs previously observed in the 9 : 1 TFE-d/H<sub>2</sub>O mixture were present. When dissolved in aqueous solutions containing 30% or 15% TFE-d, only residues 8–22 showed a sequential HN<sub>*i*</sub>/HN<sub>*i*+1</sub> NOE. When less than 15% TFE-d was used, or in pure water, even at 3°C, salmon calcitonin behaved nearly as a random coil peptide giving very limited number of NOEs and very narrow spread of

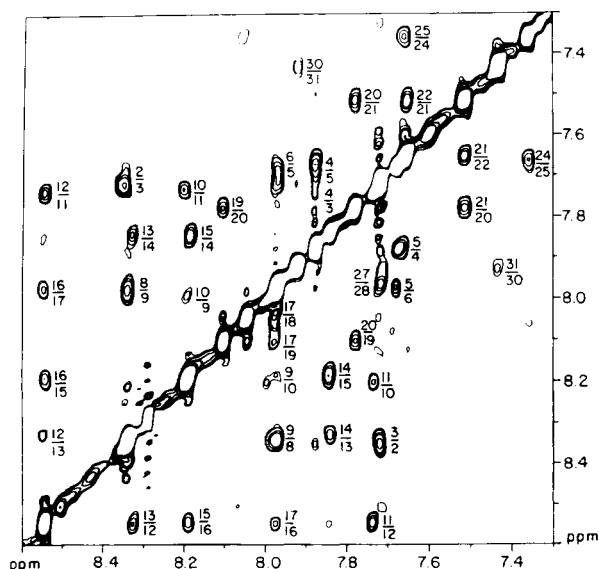


**Figure 2.** Diagonal NOESY detail showing the sequential  $\text{HN}_i/\text{HN}_{i+1}$  NOEs (in 9 : 1 TFE-d/ $\text{H}_2\text{O}$ ). The peaks are labeled with the sequential numbers of the residues involved.

chemical shifts. Even though chemical shift changed only slightly with the solvent mixture, these spectra were sometimes helpful in order to sort out ambiguities due to overlaps in the reference spectrum.

**Assignment.** The following full analysis and the subsequent distance geometry are based on the spectra of the peptide in 9 : 1 TFE-d/ $\text{H}_2\text{O}$ . Nevertheless, simpler spectra in pure TFE-d were analyzed first (data not shown). We took advantage of the fact that an  $\alpha$ -helical structure provides a characteristic pattern in the NOESY spectrum. This was applied to the  $\text{HN}/\text{HN}$  and  $\text{HN}/\text{HA}$  regions. Sequential delineation allowed us to trace the main-chain amino acids from Val 8 to Gln 20, where the connectivities stopped.

NOESY  $\text{HN}_i/\text{HN}_{i+1}$  connectivities and COSY  $\text{HN}_i/\text{HA}_i$  cross peaks were then aligned with the corresponding peaks in the HOHAHA spectrum, providing full assignment of backbone and side-chain protons of amino acids 8–20. Assignment of the spin system of Tyr 22 was made possible by the detection of intraresidual HA or HB NOEs with HD and HE protons, although no sequential  $\text{HN}_i/\text{HN}_{i+1}$  NOE or  $\text{HN}_i/\text{HA}_i$  cross peak could be detected. Two additional threonine patterns were detected in the NOESY and HOHAHA amide region. The absence of any additional  $\text{HN}_i/\text{HN}_{i+1}$  sequential or other connectivities prevented further attribution at this stage.

The two proline residues could be found due to their typical NOESY pattern. Strong NOESY connectivities from the HD protons of one proline to the HA and HD protons of Tyr 22 and to the HB proton of Arg 24 were observed. NOEs from the other proline HD protons to HA and HB protons of a threonine (Thr 31) were also identified. We thus assigned these two patterns to Pro 23 and Pro 32, respectively.

All the above assignments were then easily re-identified in the spectra of the peptide in the 9 : 1 TFE-d/ $\text{H}_2\text{O}$  mixture, due to the negligible chemical shift changes. In the amide region (Figure 2), additional sequential NOEs could be found. Amino acids within the ring and others, like Thr 21, Tyr 22, Arg 24, and Gly 30 displayed  $\text{HN}_i/\text{HN}_{i+1}$  NOEs. These connectivities showed corresponding  $\text{HN}_i/\text{HA}_i$  COSY cross peaks (Figure 3). Furthermore, all remaining amino acids showed a  $\text{HN}_i/\text{HA}_i$  COSY peak (Figure 3; except, of course, Cys 1, Pro 23, and Pro 32). A full sequential assignment was thus achieved (Table I). The summary of the NOEs used for assignment is given in Figure 4.

**Secondary Structure.** The major secondary structure feature is an  $\alpha$ -helix. Figure 5 summarizes some characteristic NOEs, e.g., the strong  $\text{HN}_i/\text{HN}_{i+1}$ ,  $\text{HA}_i/\text{HB}_{i+3}$ ,  $\text{HA}_i/\text{HN}_{i+3}$ . The unobserved peaks are missing because of the overlap or degeneracy of some resonances. A diagonal NOE pattern (Figure 4) is also typical for the  $\alpha$ -helix between residue 8 and 22. These residues also provide smaller values

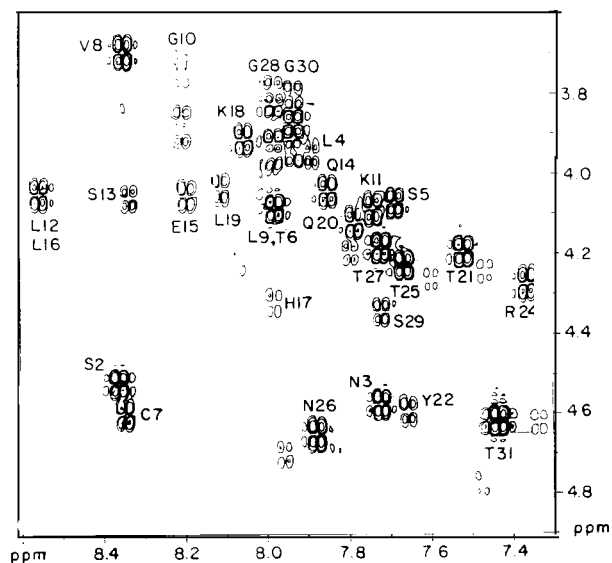


**Figure 3.** COSY detail (fingerprint region) showing the intraresidual  $\text{HN}_i/\text{HA}_i$  cross peaks (in 9 : 1 TFE-d/ $\text{H}_2\text{O}$ ).

**Table I Sequential Assignment of Salmon Calcitonin**

Amino Acid	Chemical Shift					
	HN	HA	HB	HG	HD	HE
C1		4.34	3.63 3.19			
S2	8.34	4.41	3.90 3.78			
N3	7.72	4.58	3.09 2.97		7.08 6.26	
L4	7.88	3.97	1.64	1.58	0.85 0.80	
S5	7.78	4.08	3.85			
T6	7.97	4.09	4.23	1.28		
C7	8.35	4.59	3.09			
V8	8.34	3.69	2.12	0.98 0.87		
L9	7.97	4.09	1.79 1.55	1.73	0.81	
G10	8.20	3.88 3.75				
K11	7.73	4.08	1.93	1.47	1.67	2.91
L12	8.54	4.05	1.73	1.67	0.80	
S13	8.33	4.08	3.95			
Q14	7.84	4.04	2.29 2.19	2.57		6.79 6.12
E15	8.19	4.05	2.28 2.13	2.50		
L16	8.53	4.05	1.76	1.44	0.80	
H17	7.97	4.32	3.28		7.20	8.29
K18	8.04	3.92	1.93 1.56	1.36	1.65	2.89
L19	8.11	4.03	1.85	1.55	0.82 0.78	
Q20	7.78	4.13	2.33 2.12	2.48		6.62 6.02
T21	7.52	4.19		1.09		
Y22	7.55	4.58	3.05		7.05	6.69
P23		4.27	2.17 1.78	1.95 1.88	3.74 3.33	
R24	7.36	4.27	1.88 1.76	1.62	3.10	
T25	7.66	4.23		1.13		
N26	7.88	4.65	2.72 2.67		6.91 6.12	
T27	7.71	4.19	4.23	1.13		
G28	7.97	3.93 3.84				
S29	7.72	4.33	3.88 3.77			
G30	7.92	3.91 3.83				
T31	7.42	4.61	4.16	1.12		
P32		4.44	2.13 1.79	1.98 2.02	3.68 3.79	

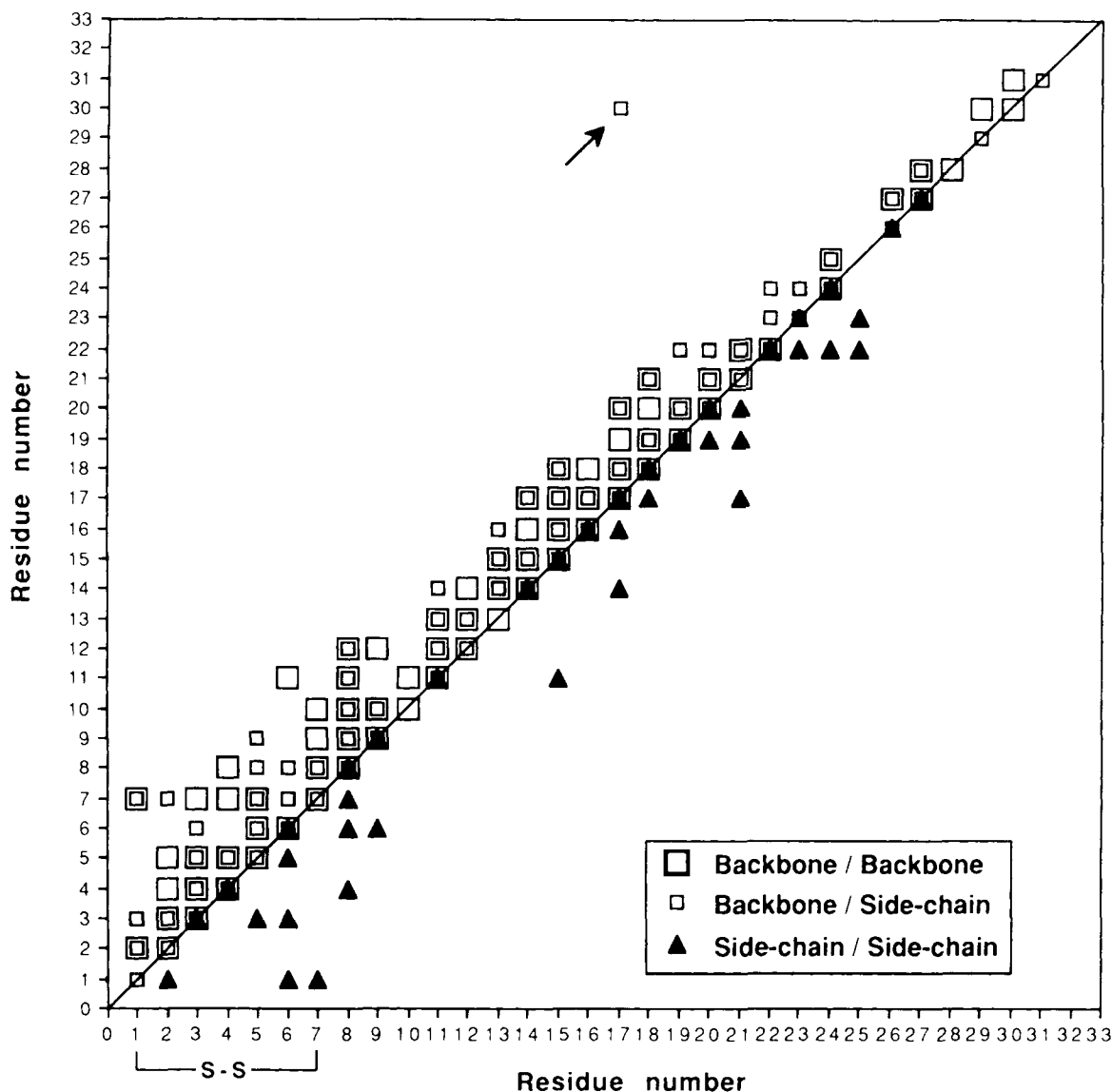


**Figure 4.** Summary of the NOEs used for the sequential assignment and identification of the secondary structure.

of coupling constants (data not shown) between HN and HA resonances than the others, and finally, only HN resonances of amino acids stabilized by hydrogen bonding in the helix exchange slowly in pure TFE.

Amino acids 1–7 are located within a conformationally constrained ring. They all show not only intraresidual and sequential NOEs, but also long-range NOEs (e.g., Thr 6 HG to Asn 3 HN). NOEs could also be detected between amino acids within the ring and the first amino acids of the  $\alpha$ -helix (e.g., Leu 4 HA, HB, and HG to Val 8 HG; Figure 4).

In the C-terminal decapeptide, only sequential NOEs were found, except for the Gly 30 HN to His

17 HB NOE and for residues 22–25 (Figure 4). This portion of the peptide shows several NOEs between these four amino acids, suggesting the formation of a loop in the last 10 residues of the C-terminus. The unique but structurally important long-range NOE between His 17 and Gly 30 was checked by NOE buildup and was also observed in the spectrum taken in 50% TFE.

#### Distance Geometry Calculations

The full sequential assignment yielded 365 NOEs (154 intraresidual, 112 sequential, and 99 long range). Their distribution is shown in Figures 4 and 5. They were converted into upper limit distances

and used together with van der Waals radii as distance constraints in the distance geometry program DISMAN. Five hundred starting structures were generated randomly. In the first runs, the hydrogen-bond distances were not specified. Inspection of the resulting structures showed, however, that the  $\text{CO}_i/\text{HN}_{i+3}$  distances in the helix were about 3 Å. In the following runs, these distances were therefore included for the residues whose HN protons were detected in TFE (Figure 5). The coupling constants were not used in the calculations because of their large experimental error. The six structures best satisfying the nmr constraints were selected and compared. They are overlayed for the minimal root mean square deviation (RMSD) for the main-chain atoms in Figure 6. The fit was made both on the whole peptide and between residues 1–22. A good RMSD ( $\text{RMDS} \leq 2$  Å) was obtained for amino acids 1–22, while substantial deviations ( $\text{RMDS} \approx 5$  Å) were observed for the C-terminal decapeptide.

## DISCUSSION

Whereas salmon calcitonin exhibits little or no structure in water, CD spectra show that the peptide, in a structure-promoting solvent like TFE, adopts a globular conformation, even if the percentage of TFE is low (Figure 1). The intensity of the 222-nm band was similar to that previously described for salmon calcitonin in the presence of lipids.<sup>15</sup> The structure of the peptide was not greatly altered by changes in pH or temperature. This was fully confirmed by nmr. We have examined a standard set of two-dimensional proton nmr spectra. All spectra were well resolved and assignment was complete (Table I).

Spectra taken in both pure TFE-d or 9 : 1 TFE-d/ $\text{H}_2\text{O}$  mixture show no significant differences in chemical shifts and NOEs for amino acids 8–20, indicating that the structure is similar, although pro-

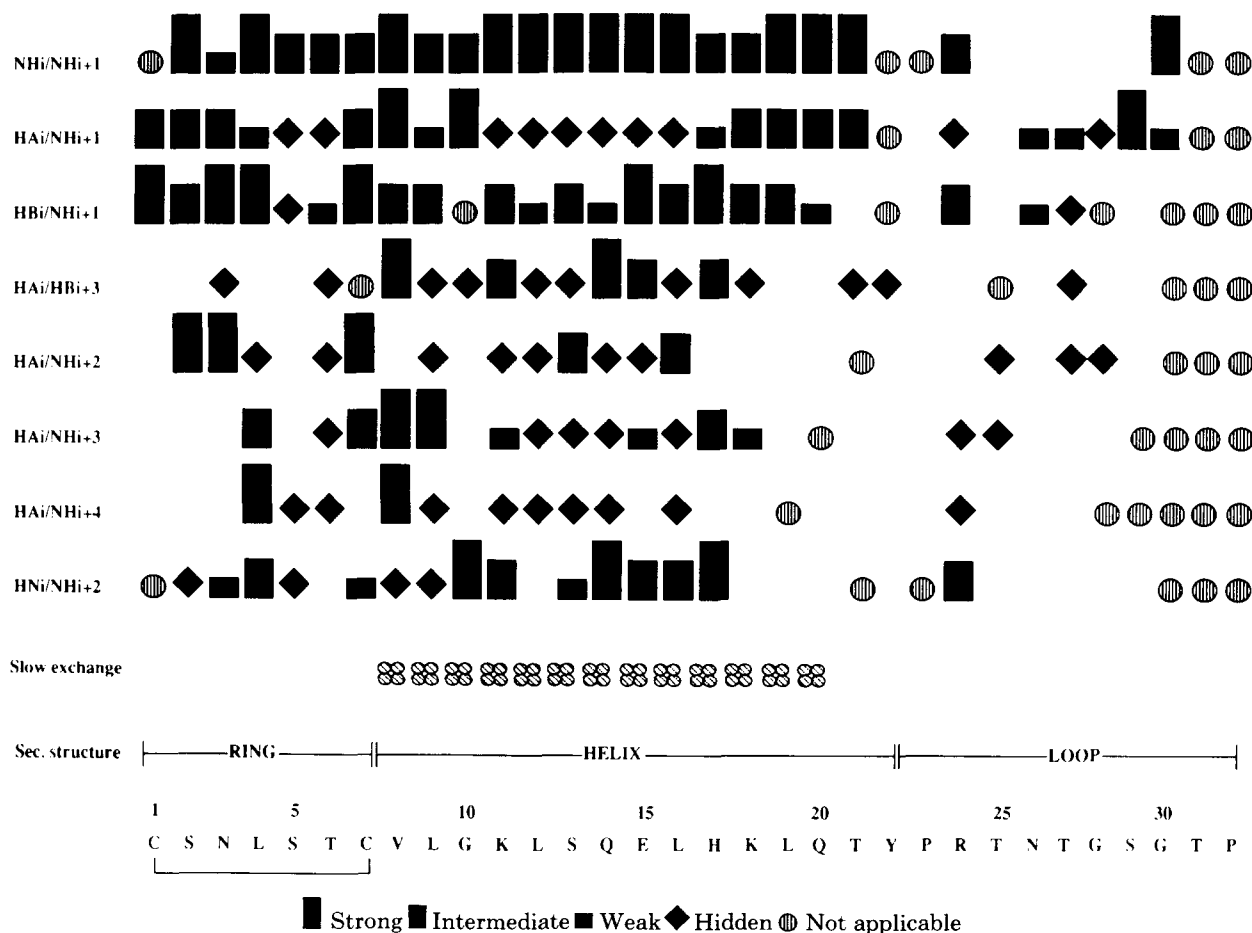


**Figure 5.** Repartition of the NOEs. A symbol connects the numbers of the residues between which a NOE was detected.



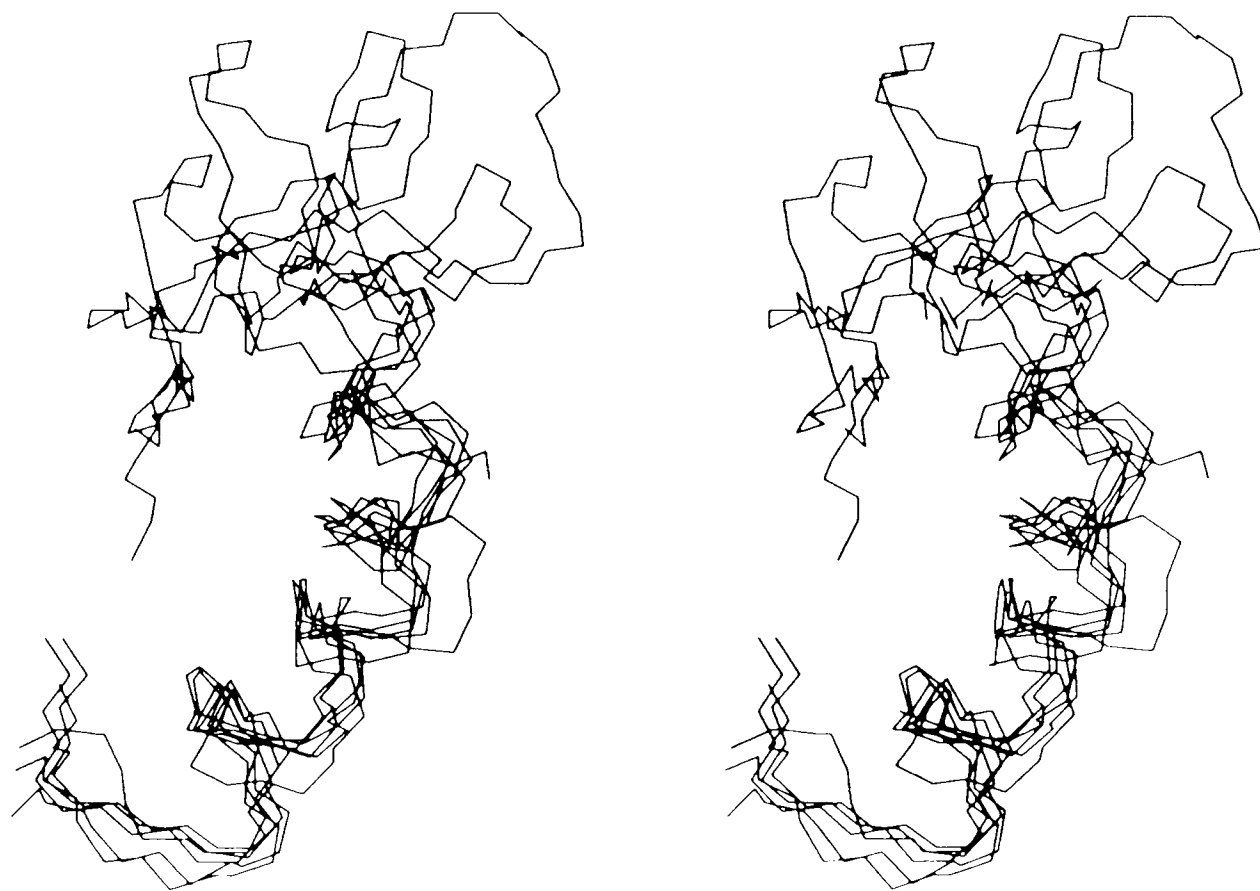


**Figure 6.** Superposition of the best six calculated structures (stereoscopic view). Residues 1–22 were fitted for minimal RMSD between the main-chain atoms.

line *cis/trans* isomerization can be detected when water is added.

Analysis of the NOESY spectrum shows that typical  $\alpha$ -helical NOEs are present for amino acids 8–22 (Figure 5). The Cys 1–Cys 7 ring is well defined and is in close association with the beginning of the helix.

In the C-terminal decapeptide, mainly sequential NOEs could be observed, indicating that this portion of the peptide is much more mobile. Nevertheless, NOEs in the Tyr 22 to Thr 25 region clearly indicate a bend in the molecule. This is confirmed by the His 17 to Gly 30 NOE and suggests that the C-terminus folds back toward the core of the molecule (Figure 6).

Another important point is to notice that the helix does not begin exactly at Val 8, but that amino acids 4–7 of the N-terminal ring are also involved in a helix (Figure 6).

The  $\alpha$ -helix, from residues 8 to 22, forms an amphiphilic helix with hydrophobic residues on one face of the peptide. This result had been previously sug-

gested since the peptide displays hydrophobic residues (mainly leucines) every three or four amino acids.<sup>16,17</sup> Moreover, this helix is slightly curved, with the hydrophobic face on the outside. These results are in agreement with the structure predicted for salmon calcitonin by Chou–Fasman analysis.<sup>4,18</sup> A previous nmr study suggested the presence of an  $\alpha$ -helix for human calcitonin<sup>19</sup> in a TFE/water mixture and for salmon calcitonin<sup>20</sup> in SDS micelles. Nevertheless, no such structure was found for salmon calcitonin in a DMSO/water mixture.<sup>5</sup> The presence of the amphiphilic helix is believed to be important for the interaction between this peptide and lipids,<sup>16</sup> but not for its biological activity. Indeed, some salmon calcitonin analogues with less helical content than the native peptide display enhanced *in vitro* activity.<sup>15</sup> The C-terminal decapeptide is known to be important for biological activity. The fragment salmon calcitonin (1–23) peptide has only 0.25% of the activity of the native peptide, although the  $\alpha$ -helix is present.<sup>21</sup> Our study shows that although the C-terminus is substantially more mobile

than the (1-23) N-terminal region, it still has a defined structure and interacts with the  $\alpha$ -helix.

*Note Added in Proof.* A recent study (A. L. Breeze, T. S. Harvey, R. Bazzo and I. D. Campbell, Biochemistry, in press) shows that the human Calcitonin gene-related peptide assumes in solution a conformation almost identical to that of Salmon Calcitonin.

## REFERENCES

1. MacIntyre, I. (1986) *Clin. Trials J.* **23**(suppl. 1), 13-18.
2. Epand, R. M. (1983) *Mol. Cell. Biochem.* **57**, 41-47.
3. Moe, G. R., Miller, R. J. & Kaiser, E. T. (1983) *J. Am. Chem. Soc.* **105**, 4100-4102.
4. Merle, M., Lefevre, G. & Milhaud, G. (1979) *Biochem. Biophys. Res. Commun.* **87**, 455-460.
5. Motta, A., Goud, N. & Temussi, P. A. (1989) *Biochemistry* **28**, 7996-8002.
6. Merrifield, R. B. (1963) *J. Am. Chem. Soc.* **85**, 2149-2154.
7. Stewart, J. P. & Young, J. D. (1984) in *Solid Phase Peptide Synthesis*, Pierce Chemical Co., Rockford, IL.
8. Tam, J. P., Heath, W. F. & Merrifield, R. B. (1983) *J. Am. Chem. Soc.* **105**, 6442-6455.
9. Bree, A. & Lyons, L. E. (1956) *J. Chem. Soc.* 2658-2670.
10. Wüthrich, K. (1986) *NMR of Proteins and Nucleic Acids*, Wiley, New York.
11. Rance, M., Sorensen, O. W., Bodenhausen, G., Wagner, G., Ernst, R. R. & Wüthrich, K. (1983) *Biochem. Biophys. Res. Commun.* **117**, 479-485.
12. Rance, M. (1987) *J. Magn. Reson.* **74**, 557-564.
13. Jeener, J., Meier, B. H., Bachmann, P. & Ernst, R. R. (1979) *J. Chem. Phys.* **71**, 4546-4553.
14. Chen, Y. H., Yang, J. T. & Martinez, H. M. (1972) *Biochemistry* **11**, 4120-4131.
15. Epand, R. M., Epand, R. F., Orlowski, R. C., Seyler, J. K. & Colescott, R. L. (1986) *Biochemistry* **25**, 1964-1968.
16. Epand, R. M., Epand, R. F., Orlowski, R. C., Schlueter, R. J., Boni, L. T. & Hui, S. W. (1983) *Biochemistry* **22**, 5074-5084.
17. Moe, G. R. & Kaiser, E. T. (1985) *Biochemistry* **24**, 1971-1976.
18. Chou, P. Y. & Fasman, G. D. (1974) *Biochemistry* **13**, 222-245.
19. Doi, M., Kobayashi, Y., Kyogoky, Y., Takimoto, M. & Goda, K. (1989) in Rivier J. E. & Marshall, G. R., Eds., *Proceedings of the 11th American Peptide Symposium*, La Jolla, CA.
20. Motta, A., Castigione-Morelli, M. A., Goud, N. & Temussi, P. A. (1990) Poster presentation at the Second Naples Workshop.
21. Epand, R. M., Stahl, G. L. & Orlowski, R. C. (1986) *Int. J. Peptide. Res.* **27**, 501-507.

Received July 18, 1990

Accepted September 7, 1990